Scientific Research Publishing

Advances in Biological Chemistry, 2021, 11, 30-51
https://www.scirp.org/journal/abc
ISSN Online: 2162-2191
ISSN Print: 2162-2183

Synthesis, Characterization, Antimicrobial and DNA Binding Studies of a Tetradentate N_2O_2 Amino Acid Schiff Base and Its Coordination Compounds

Temitayo O. Aiyelabola[1*], Daniel P. Otto[2], Johan H. L. Jordaan[2], Ezekiel O. Akinkunmi[3], Idowu Olawuni[4]

[1]Department of Chemistry, Obafemi Awolowo University, Ile-Ife, Osun State, Nigeria
[2]Research Focus Area for Chemical Resource Beneficiation, Laboratory for Analytical Services, North-West University, Potchefstroom, South Africa
[3]Department of Pharmaceutics, Obafemi Awolowo University, Ile-Ife, Osun State, Nigeria
[4]Department of Biochemistry and Molecular Biology, Obafemi Awolowo University, Ile-Ife, Osun State, Nigeria
Email: *taiyelabola@gmail.com, *taiyelabola@oauife.edu.ng, Johan.Jordaan@nwu.ac.za, Daniel.Otto@nwu.ac.za, eoakinmi@oauife.edu.ng, olawunij@gmail.com

How to cite this paper: Aiyelabola, T.O., Otto, D.P., Jordaan, J.H.L., Akinkunmi, E.O. and Olawuni, I. (2021) Synthesis, Characterization, Antimicrobial and DNA Binding Studies of a Tetradentate N_2O_2 Amino Acid Schiff Base and Its Coordination Compounds. *Advances in Biological Chemistry*, **11**, 30-51.
https://doi.org/10.4236/abc.2021.111004

Received: December 13, 2020
Accepted: February 7, 2021
Published: February 10, 2021

Abstract

Aminoethanoic acid undergoes condensation with 1,4-benzenedicarboxaldehyde to form an O, N, N, O donor Schiff base, *N,N′*-di(carboxymethylene) terephthalaldehyde, Ligand L. Coordination compounds of this Schiff base using Ni (II), Cu (II), VO (IV) and Co (II) were then obtained *in-situ*. The Schiff base and the complexes were evaluated for their antimicrobial and DNA binding abilities. Molecular docking studies of the ligand and synthesized compounds were also carried out. Evidence for the formation of the Schiff base coordination compounds and the coordinating atoms was obtained from ^{1}H NMR, infrared and ultraviolet spectral data, EDX, EDTA complexometric titration and magnetic susceptibility measurement. The results obtained are consistent with octahedral geometry for Ni (II) complex, the metal ion coordinating to one molecule of Ligand L and with additional coordination with two oxygen atoms of two molecules of the solvent. A square-planar geometry was suggested for both Co (II), and Cu (II) complexes and a five-coordinate, square pyramidal geometry for the VO (IV) complex. The results further indicated that the carboxylic acid of Ligand L was not deprotonated both in the free base and also the complexes. In addition, the results showed that Compound 2 elicited the best antimicrobial activity potential. Generally, the compounds exhibited considerable good affinity to CT-DNA.

Keywords

CT-DNA, DNA Binding, Antimicrobial, Coordination Compound, Molecular Docking, Schiff Base

1. Introduction

Schiff bases and their coordination compounds have been extensively investigated and employed in areas that include magneto chemistry, non-linear optics, photo physical studies, catalysis materials chemistry and medicinal chemistry [1] [2] [3] [4] [5]. Tetradentate Schiff bases with N_2O_2 donor atoms are well known to coordinate with various metal ions and have attracted a great deal of interest in recent years due to their rich coordination chemistry [6] [7] [8] [9] [10]. Nevertheless, considerable effort is still being invested in the development of these compounds as new chelating agents as a result of their versatility [6] [7] [8] [9] [10]. A group of such Schiff bases is derived from amino acids [11] [12] [13] [14]. These complexes act as good chelating agents as such there are many interesting studies on them. They have been used as ligands and their complexes found usage in medicinal chemistry including potential cytotoxic, antibacterial and anticancer agents [11] [12] [13] [14]. The investigation of drug-DNA interaction is of importance for understanding the molecular mechanism of drug action and for the design of specific DNA-targeted drug due to their importance in cancer therapy, design of new types of pharmaceutical molecules and molecular biology [5]-[19].

However, few studies were carried out concerning the interaction of DNA with Schiff base amino acid complexes [20]. Interaction with DNA is accepted to be the cellular target of mechanism of activity of some coordination compounds used as therapeutic agents [21]. Although coordination compounds are successfully being used in cancer therapy and several other therapies, however, there are reported cases of some side effects and resistance [21]. Therefore there is a need for new approaches to circumvent these drawbacks and pave way for potent drug therapies. It has been shown from previous reports that coordination of biologically important molecules enhances their ability to permeate the cell wall of certain microbes [22] [23] [24] [25] [26]. As a consequence, they may interact with biomolecules, such as nucleic acids and proteins, within the interior of the microbe. They have been reported to bind to DNA nitrogen bases resulting in an alternation of the normal DNA transcription regulation thereby disrupting genome and cellular processes [27]. In most cases, the DNA-interaction with complexes depends on the structure and stability of the complexes as well as the nature of their ligands. This interaction may take place via the formation of covalent bonds or in a non-covalent manner (intercalation, electrostatic interactions and/or groove-binding) or may lead to cleavage of the DNA-helix [28].

Currently there is a global shortage of efficient antimicrobials to successfully

combat drug resistant pathogens. There is therefore a need for new or lead compounds as antibiotics [27]. Although, Schiff base of 1,4-benzenedicarboxaldehyde and some amino acids, including aminoethanoic acid and their coordination compounds have been synthesized and characterized [29]. However, the use of different synthetic route and varying reaction conditions, have been shown, may lead to differences in the resultant Schiff base and coordination compounds obtained [30]. Therefore, this led to our synthesizing a Schiff base using 1,4-benzenedicarboxaldehyde (**Figure 1**) and aminoethanoic acid (**Figure 2**) and its coordination compound. The Schiff base was characterized using proton NMR, uv-vis and infrared spectroscopy. The coordination compounds were obtained using nickel (II), copper (II), vanadyl (IV) and cobalt (II) ion. The resultant coordination compounds were characterized using uv-vis and infrared spectroscopy, energy-dispersion X-ray spectroscopy EDX, EDTA complexometric titration and magnetic susceptibility measurement. The complexes were evaluated for their *in vitro* antimicrobial and DNA binding ability. Additionally, molecular docking of the ligand and synthesized compounds was also carried out to determine their binding affinity and sites of interaction.

2. Materials and Method

All starting materials and solvents used were purchased from Aldrich and Fluka and were used without further purification. The melting points were determined on a Gallenhamp melting point apparatus and are uncorrected. The infrared spectra were recorded in the region 4000 - 499 cm^{-1} on a Fourier-Transform infrared spectrophotometer. Electronic spectra were measured on a Varian Cary 50 ultraviolet-visible spectrophotometer the measurements were made from 200 to 800 nm. Magnetic susceptibility measurements were carried out at room temperature, using a Sherwood scientific balance with $[HgCo(SCN)_4]$ as standard. EDX analyses were obtained using Shimadzu Ray ny EDX 720 The proton NMR was recorded on a Bruker spectrophotometer model ultra shield at 600 MHz in $CHCl_3$-d_6 with TMS as internal standard. Screening of the compounds for their antimicrobial activity was carried out using disc diffusion method. The

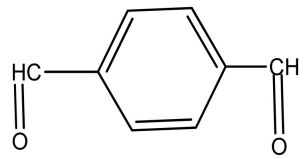

Figure 1. 1,4-benzenedicarboxaldehyde.

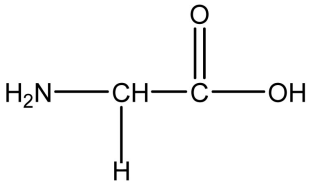

Figure 2. Aminoethanoic acid.

compounds were synthesized according to adaptation of established procedure described in literature [31]. The equations of the reactions are given in Equations (1)-(5).

$$C_8H_8O_2 + 2C_2H_5NO_2 \rightarrow C_{12}H_{12}N_2O_4 \quad \text{Ligand } \mathbf{L} \tag{1}$$

Coordination compounds:

$$NiCl_2 + C_8H_8O_2 + 2C_2H_5NO_2 \rightarrow \left[Ni\mathbf{L}(S)_2\right] \quad \text{Compound } \mathbf{1} \tag{2}$$

$$CuCl_2 + C_8H_8O_2 + 2C_2H_5NO_2 \rightarrow \left[Cu\mathbf{L}\right] \quad \text{Compound } \mathbf{2} \tag{3}$$

$$VOSO_4 + C_8H_8O_2 + 2C_2H_5NO_2 \rightarrow \left[VO\mathbf{L}\right] \quad \text{Compound } \mathbf{3} \tag{4}$$

$$CoCl_2 + C_8H_8O_2 + 2C_2H_5NO_2 \rightarrow \left[Co\mathbf{L}\right] \quad \text{Compound } \mathbf{4} \tag{5}$$

where 1,4-benzenedicarboxaldehyde = $C_8H_8O_2$; Aminoethanoic acid = $C_2H_5NO_2$; Ligand **L** = $C_{12}H_{12}N_2O_4$; S = solvent.

2.1. Syntheses of Coordination Compounds

2.1.1. Synthesis of Ligand L

A solution of aminoethanoic acid (1.56 g, 0.02 M) in absolute ethanol was added drop-wise to a stirring solution of 1,4-benzenedicarboxaldehyde (1.37 g, 0.01 M)) in 150 ml absolute ethanol and refluxed for 4 h after the addition of 4 drops of acetic acid. A yellow precipitate was obtained, which was recrystallized using chloroform–ethanol mixture (70/30 v/v), washed, filtered and dried in a vacuum oven at 60˚C to give ligand **L**. Yield: 1.47 g (58.20%), M.pt: 126˚C - 127˚C.

^{1}H NMR (600 MHz) $CHCl_3$-d_6, (δ ppm): 7.24 (s, 2H, HC=N), 2.13 (d, 4H, J= -CH_2), 8.01 (m, 4H), 10.09 (s, 2H, -OH).

IR (cm^{-1}): 3177 ν (O-H), 1689 ν (C=N), 1586 ν (C ⎓ N) + ν (C ⎓ C), 1518 ν (C-N) + δ (C-H), 1412 δ (C-H) + ν (C ⎓ N), 1334 δ (C-H) + ν (C ⎓ N), 1117 ν (C-N), 1038 ν (C-OH); Uv-Vis (nm): 202, 220 and 345.

2.1.2. Compound 1

A solution of $NiCl_4$ (1.72 g, 0.01 M) in absolute ethanol was added to a stirring solution of 1,4-benzenedicarboxaldehyde (1.35 g, 0.01 M) in 150 ml of absolute ethanol into which ethanolic solution of aminoethanoic acid (1.52 g, 0.02 M) was added drop-wise and refluxed for 4 h after the addition of 4 drops of acetic acid. A pale green precipitate was obtained, which was recrystallized using ethanol–water mixture (70/30 v/v), washed, filtered and dried in a vacuum oven at 60˚C to give compound **1**. Yield: 2.01 g (65.80%), M.pt: 201˚C - 202˚C (d); metal composition (%): calc.19.28; found: 19.86. The complex was sparingly soluble in ethanol, methanol but soluble in water.

IR (cm^{-1}): 1581 ν (C ⎓ N) + ν (C ⎓ C), 1402 δ (C-H) + ν (C ⎓ N), 1039 ν (C-OH), 619 ν (M-N), 592 and 557 ν (M-O); Uv-Vis (nm): 232, 334 550 and 563.

2.1.3. Compound 2

A solution of copper (II) chloride (1.36 g, 0.01 M) in absolute ethanol and 20 ml

solution of aminoethanoic acid (1.54 g, 0.02 M) in absolute ethanol were added drop-wise to a stirring solution of 1,4-benzenedicarboxaldehyde (1.36 g, 0.01 M) in 150 ml absolute ethanol and refluxed for 4 h after the addition of 4 drops of acetic acid. A blue precipitate was obtained, which was recrystallized using ethano-water mixture (70/30 v/v), washed, filtered and dried in a vacuum oven at 60˚C to give compound **2**. Yield: 2.92 g (72.54%). M.pt: 167˚C - 169˚C (d); metal composition (%): calc.20.42; found: 21.56. The complex was sparingly soluble in ethanol, methanol and water.

IR (cm^{-1}): 3173 ν (O-H), 1592 ν (C = N) + ν (C = C), 1516 ν (C-N) + δ (C-H), 1412 δ (C-H) + ν (C = N), 1334 δ (C-H) + ν (C = N), 1117 ν (C-N), 1042 ν (C-OH), 608 ν (M-N), 556 ν (M-N); Uv-Vis (nm): 225, 290, 523 and 556.

2.1.4. Compound 3

A solution of vanadyl sulphate (1.72 g, 0.01 M) was added to a stirring solution of 1,4-benzenedicarboxaldehyde (1.37 g, 0.01 M) in 170 ml. A solution of aminoethanoic acid (1.54 g, 0.02 M) in absolute ethanol was also added simultaneously drop-wise absolute. The resultant mixture was refluxed for 4 h after the addition of 4 drops of acetic acid. A bluish green precipitate was obtained, which was recrystallized using ethanol–water mixture (70/30 v/v), washed, filtered and dried in a vacuum oven at 60˚C to give **3**. Yield: 2.18 g (68.40%), M.pt: 232˚C - 233˚C; metal composition (%): calc.16.98; found: 17.54. The complex was sparingly soluble in ethanol, methanol and water.

IR (cm^{-1}): 3195 ν (O-H), 1615 ν (C=N), 1575 ν (C = N) + ν (C = C), 600 ν (M-N), 534 ν (M-O); Uv-Vis (nm): 240, 332, 450, 628 and 847.

2.1.5. Compound 4

An ethanolic solution of cobalt (II) chloride (1.54 g, 0.01 M) was added to a stirring solution of 1,4-benzenedicarboxaldehyde (1.37 g, 0.01 M) in 150 ml absolute ethanol. An ethanolic solution of aminoethanoic acid (1.52 g, 0.02 M) was added drop-wise simultaneously and refluxed for 4 h after the addition of 4 drops of acetic acid. A pink precipitate was obtained, which was recrystallized washed and filtered and dried in a vacuum oven at 60˚C to give **4**. Yield: 1.90 g (61.82%), M.pt: 250˚C - 252˚C (d); metal composition (%): calc.18.89; found: 19.34. The complex was sparingly soluble in ethanol, methanol but soluble in water.

IR (cm^{-1}): 3245 ν (O-H), 1592 ν (C = N) + ν (C = C), 1408 δ (C-H) + ν (C = N), 1039 ν (C-OH), 624 ν (M-N), 576 ν (M-O); Uv-Vis (nm): 259, 349, 512 and 735.

2.2. Antimicrobial Methodology

The organisms used were five Gram-positive and three Gram-negative bacteria and two fungi. These were *Staphylococcus aureus* (ATCC 29213), *Staphylococcus epidermidis* (clinical strain), *Bacillus subtilis* 12 (NCIB 3610), *Bacillus subtilis* 82 (NCIB 6349), *Clostridium sp.* (NCIB 532), *Klebsiella pneumonia* (clinical strain), *Pseudomonas aeruginosa* (ATCC 27853), *Escherichia coli* (ATCC 25922), *Candida albicans* (ATCC 24433) and *Candida pseudotropicalis* (NCYC 6), re-

spectively. The agents were dissolved in water at room temperature or hot water as appropriate to give a concentration of 40 mg/ml. The resulting solutions were used to soak sterile Whatman No 2 discs (diameter = 6 mm) and allowed to dry in an oven at 50˚C. The discs were then used to determine antibacterial and antifungal activities as previously described by Aiyelabola *et al.* 2012 [32]. Discs of imipenem and chlorhexidine were used as positive controls for bacteria and fungi respectively. Zones of inhibition were used as indices of antimicrobial actions.

2.3. DNA Binding Experiments

2.3.1. Methodology for DNA Binding Using Absorption Spectroscopic Studies

All the experiments involving the interaction of the complexes with DNA were carried out in Tris-HCl buffer (50 mM, pH 7.2). A solution of calf thymus DNA in the buffer gave a ratio of UV absorbance at 260 and 280 nm of about >1.79, indicating that the DNA was sufficiently free from protein contamination [33] [33]. The concentration of DNA was determined by monitoring the UV absorbance at 260 nm using ε 260 = 6600 $mol^{-1} \cdot cm^2$. The stock solution was stored at 4˚C and used within only one day. Spectrophotometeric titration experiment was performed by:

1) Maintaining a constant DNA concentration (1.2 - 1.4 × 10^{-4} M) in the presence of each complex at diverse [complex]/[DNA] mixing ratios (=R) and;

2) Maintaining metal complex concentration constant (2.0 × 10^{-4} - 1.8 × 10^{-4} M) in the presence of increasing concentration of CTDNA at diverse [DNA]/[complex] mixing ratio (=R).

The absorption due to free CT-DNA or metal complex was eliminated by adding the corresponding equimolar CT-DNA/metal complex to pure buffer solution in the reference compartment and the resulting spectra were considered to result from the metal complex-DNA and the DNA-metal complex aggregates. From the absorption data, the intrinsic binding constant (K_b) was determined by plotting [DNA]/($\varepsilon_a - \varepsilon_f$) vs. [DNA] according to the Wolfe-Shimer equation:

$$[\mathrm{DNA}]/(\varepsilon_a - \varepsilon_f) = [\mathrm{DNA}]/(\varepsilon_b - \varepsilon_f) + 1/[K_b(\varepsilon_a - \varepsilon_f)]$$

where [DNA] is the concentration of DNA in base pairs,

ε_a, ε_f and ε_b are the apparent, free and fully bound complex absorption coefficients, respectively.

Furthermore, ε_f was determined from the calibration curve of the isolated metal complex; following the Beer's law, ε_a was determined as the ratio between the measured absorbance and the metal (II) complex concentration, A_{obs}/[complex] [28]. The data were fitted to the above equation with a slope equal to $1/(\varepsilon_b - \varepsilon_f)$ and y-intercept equal to $1/[K_b(\varepsilon_b - \varepsilon_f)]$ and K_b was obtained from the ratio of the slope to the intercept [35] [36].

2.3.2. Viscosity Experiments for Interaction of the Prepared Complexes with DNA

Viscosity measurements were carried out using an Oswald microviscometer,

maintained at constant temperature at 25˚C. The flow times were recorded for different concentrations of the complex (10 - 50 μM), maintaining the concentration of DNA constant (0.5 mM). The average value of the three measurements was used to determine the viscosity of the samples. The buffer flow time in seconds was recorded as t^o. The relative viscosities for DNA in the presence (η) and absence (η_0) of the complex were calculated using the relation $\eta = (t - t^o)/t^o$. Where, t is the observed flow time in seconds and the values of the relative viscosity (η/η_0) were plotted against 1/R (R = [DNA]/[Complex]) [37].

3. Result and Discussion

3.1. Ligand L

3.1.1. ^{1}H NMR

The proton NMR of ligand **L** provided evidence for the formation of the Schiff base as a result of the signal observed at 7.24 ppm, which was absent in that of the starting material [38] [39] [40]. This is assignable to the azomethine proton (-N=CH), which resonated downfield, than expected, due to its sp^2 hybridized methine carbon been shielded as a result of conjugation with the lone pair of electrons on the azomethine nitrogen atom [38] [39] [40] [41]. This is supported by reports from previous studies [38] [39] [40] [41]. Further buttressing the formation of a Schiff base was the presence of a doublet at 2.13 and 2.40 ppm ascribed to the methylene protons, from previous studies this multiplicity suggests that the molecule is not completely planar and may be slightly bent. The signal obtained downfield at 10.09 ppm was ascribed to the hydroxyl proton of the carboxylic acid moiety, thus indicating that it was not deprotonated and also suggests the presence of hydrogen bond. The aromatic protons resonated as a multiplet at 8.01 ppm [38] [39] [40] [41].

3.1.2. Fourier-Transformed Infrared

Evidence of the formation of the Schiff base was suggested by the azomethine absorption frequency band at 1689 cm^{-1} [38] [39] [42]. Supporting this was the absence of the N–H and carbonyl stretching frequencies which were present in the starting material. A broad band in the shape of a trough at 3177 cm^{-1} ascribed to the ν (O-H). This was observed at lower frequency than that expected. It is suggested that this may be as a result of intra-molecular hydrogen bonding [38] [39] [42]. Further supporting this are frequencies observed at 2903 and 2615 cm^{-1} [38] [39] [42]. Corroborating this further was the ν (C-OH) at 1038 cm^{-1}. Further evidence for the formation of the Schiff base was given by bands observed at 1586, 1518 and 1334, which are assignable to ν (C-N) + ν (C-C), ν (C-N) + δ (C-H) and δ (C-H) + ν (C-N). Additional observed absorption frequencies include 1412, 1400 and 1117 nm ascribable to δ (CH_2), ν (C=O) and ν (C-N) [38] [39] [42].

3.1.3. Electronic transitions

The ultraviolet spectrum of ligand **L** exhibited bands at 202, 220 and 345 nm and

are assigned to $\pi \rightarrow \pi^*$ and $n \rightarrow \pi^*$ of the major chromophores of the ligand the aromatic, C=N and carboxylic acid substituents [38] [39] [43].

3.2. Coordination Compounds

3.2.1. Compound 1

Evidence of coordination and formation of the Schiff base was inferred by the shift in the δ (C-H) + ν (C = N) absorption frequency observed at 1402 cm^{-1} relative to what was obtained for the ligand in the FTIR spectrum of compound **1** [38] [39] [42]. The appearance of the ν (C = N) + ν (C = C) at 1581 cm^{-1} stands as further confirmation to the formation of the Schiff base [38] [39] [42]. Corroborating this was the absence of the carbonyl and amine stretching frequencies which were present in the starting material. No clear well defined band was observed for the hydroxyl moiety, only weak sharp extended bands were observed in this region [38] [39] [42]. However, the band observed at 1039 cm^{-1} which is assignable to the ν (C-OH), points to the fact that the carboxylic acid moiety was not deprotonated [38] [39] [42] [44] [45]. Further evidence for coordination of the metal ion with the ligand was the observance of the metal nitrogen stretching frequency at 619 cm^{-1} and the metal oxygen stretching frequency 592 cm^{-1} and 557 cm^{-1} [42]. This therefore, suggests that cyclization occurred in the coordination sphere of the metal ion.

The electronic spectrum of this complex showed two sets of bands. In the ultraviolet region, two intense bands were observed at 232 and 334 nm. The other set of bands were observed in the visible region as a well resolved band at 563 nm and a shoulder at 550 nm. These were assigned to spin allowed transitions of $^3A_{2g}$ (F) $\rightarrow$ $^5T_{1g}$ (F) and $^3A_{2g}$ (F) $\rightarrow$ $^5T_{1g}$ (P) suggestive of an octahedral geometry. The magnetic moment of 2.96 BM indicated two unpaired electrons per nickel ion, further validates an octahedral geometry for the complex [46] [47].

3.2.2. Compound 2

The FTIR infrared spectrum for the copper (II) complex exhibited a stretching frequency at 3173 cm^{-1} ascribed to the ν (O-H) of the carboxylic acid, observed at lower frequency as a result of hydrogen bond. This was supported with the observed broad bands at 2593, 2158, 2149 cm^{-1} [38] [39]. Corroborating this further was the band at 1042 cm^{-1}, assigned to the ν (C-OH) [38] [39] [42]. Corroborating this was the absence of the carbonyl and amine stretching frequencies which were present in the starting material, thus formation of the Schiff base maybe suggested. Evidence for coordination and formation of the Schiff base was provided in the shifts observed for the ν (C-N) + ν (C = C) at 1592 cm^{-1} compared with the synthesized ligand **L.** Corroborating the formation of the Schiff base was the appearance of bands at 1516 and 1117 cm^{-1} which are ascribable to ν (C-N) + δ (C-H) and ν (C-N) respectively [38] [39] [42]. There was no significant shift in the frequencies observed for bands observed at 1412 cm^{-1} and 1334 cm^{-1}, which are attributable to δ (CH_2) and δ (C-H) + ν (C-N), in comparison with that obtained with the ligand [38] [39] [42]. Further evidence

and support to the N_2O_2 assignment of the proposed coordination sites is further suggested by the appearance of medium bands at 608 cm^{-1} and 556 cm^{-1} which could be attributed to ν(Cu-N) and ν(Cu-O), respectively [42] [48] [49] [50].

The electronic spectrum of the Cu (II) complex elicited one intense band and a shoulder at 225 and 290 nm in the ultraviolet region. In the visible region however a well resolved band was observed at 523 nm and a weak band at 556 nm. This may be attributed to $^2B_1 \rightarrow {}^2A_1$ and $^2E \rightarrow {}^2A_1$ transition. Its magnetic moment value of 2.40 BM is indicative of a mononuclear four coordinate geometry. This therefore suggests a square planar geometry for this complex. This is in agreement with that proposed by previous workers [46] [47].

3.2.3. Compound 3

The FTIR spectrum of this complex exhibited absorption frequency at 1615 cm^{-1} suggestive of the formation and coordination of the lone pair of electrons of the azomethine nitrogen. A sharp band observed at 3195 cm^{-1} ascribable to the ν (O-H) of the carboxylic acid. A medium band observed at 1575 cm^{-1} attributable to ν(C-N) + ν(C = C) stretching frequency, suggests the formation of the Schiff base. The appearance of bands at 500 and 634 cm^{-1} assigned to the ν(V-N) and ν(V-O) further corroborates the formation of the coordination compound. The spectrum also exhibited a signal at 980 cm^{-1} attributable to the v (V=O). [51] [52]

The ultraviolet region of the electronic spectrum of the VO (IV) complex of ligand L displayed two bans one intense and a weak band at 240 and 332 nm. These were assigned to intra-ligand transition. The visible spectrum of the complex exhibitedtwo broad at bands 450 and 628 nm ascribable to $^2B_2 \rightarrow {}^2E_1$ and $^2B_2 \rightarrow {}^2B_1$ transitions respectively. This is indicative of a square pyramidal geometry [46] [47]. From previous reports a broad band suggests possibility of pseudoaromatization of the rings around the vanadium ion when the azomethine N atoms are bridged with aromatic groups, with the d^1 electron of the vanadyl ion delocalised into the ring system. The magnetic moment of 1.79 BM obtained for the complex further supports the square pyramidal geometry [46] [47].

3.2.4. Compound 4

The infrared spectrum for the cobalt (II) complex exhibited a stretching frequency at 3245 cm^{-1} ascribed to the ν (O-H) of the carboxylic acid [38] [39]. Evidence of coordination and formation of the Schiff base was observed in the shift in the δ(C-H) + ν(C = N) absorption frequency at 1408 cm^{-1} relative to ligand **L** [42]. Supporting this was the appearance of the ν(C-N) + ν(C = C) stretching frequency band at 1592 cm^{-1}. Corroborating this is the absence of the carbonyl and amine stretching frequencies which were present in the starting material. The band observed at 1039 cm^{-1} and assigned to the ν(C-OH). Further evidence for coordination of the metal ion with that of the ligand is the observance of the metal nitrogen stretching frequency at 624 cm^{-1} ν(M–N) and the metal oxygen stretching frequency 576 cm^{-1} [53].

The electronic spectrum of compound **4** elicited two bands in the ultraviolet region: an intense one at 340 nm and a shoulder at 259 nm. Both are associated to the $\pi \rightarrow \pi^*$ and $n \rightarrow \pi^*$ intra-ligand transitions respectively. On the other hand the visible region exhibited two bands at 512 nm and 735 nm corresponding to $^2A_1 \rightarrow {}^2B_2$ and $^2A_1 \rightarrow {}^2E_1$ respectively [46] [47]. This is suggestive of a square planar geometry. It exhibited a magnetic moment of 2.45 BM which further corroborates its square planar [54].

Based on the results obtained for the syntheses of the Schiff base **L** and its coordination compounds, compounds **1** - **4**, it may be inferred that contrary to the results obtained by previous workers on similar Schiff base of 1,4-benzenedicarboxaldehyde and 2-aminoethanoic acid in which the carboxylic acid was deprotonated, in this case it was not [29]. In their publication Patel and co-workers reported the synthesis of the Schiff base, *N,N*′-di(carboxymethylene)terephthalaldehydediimine via the condensation reaction between 1,4-benzenedicarboxaldehyde and 2-aminoethanoic acid. The results they obtained suggested that the carboxylic acid end was deprotonated to give a carboxylate ester. Since our reaction conditions for the formation of the base is marked different from theirs, interesting differences may therefore, become evident, if one compares our data with that obtained by these authors [29]. Our hypothesis on the protonated carboxylic acid moiety is supported by the chemical shift observed at 10.09 ppm assignable to the hydroxyl proton of the carboxylic acid of the free base in its proton NMR. Further evidence confirming the non-deprotonation of the carboxylic acid end of the base and the formation of Schiff base was the observance, in the infrared spectra of the coordination complexes, of the hydroxyl stretching frequency and also the ν (C-OH) in some cases. This therefore supports the proposed monomeric nature of the coordination complexes as opposed to the proposed polymer structure observed in previous studies. This may be ascribed to the differing route employed in the syntheses of the coordination complexes. In this instance the coordination complexes were formed *in-situ*. Further lending credence to this proposed monomeric structure is the fact that sodium hydroxide is sparingly/partially soluble in absolute ethanol as such it not could have ionized completely in absolute ethanol. However, condensation of 1,4-benzenedicarboxaldehyde and 2-aminoethanoic acid with aqueous sodium hydroxide in 50/50, v/v aqueous ethanol afforded a white precipitate as the major product and a pale yellow precipitate as a minor product. Infrared analyses suggested carboxylate formation in the former, indicating deprotonation of the carboxylic acid end. On the other hand it suggested that in the latter, this was not deprotonated. No significant shift was observed for some bands in the infrared spectrum of the coordination compounds in comparison with the ligand. The reason for this is not quite evident but we propose that this may be as a result of cyclization that occurred within the coordination sphere of the metal ions. This it is suggested may lead to the structure of the coordination compounds to be more defined, which may result in the bonds to be less elastic in comparison with those of the free base. Fundamentally the electronic spectra

of the compounds **1** - **4** showed two intense bands in the ultraviolet region with maxima at ~225 and ~300 nm. From literature data the higher energy band may be attributed to intra-ligand $\pi \rightarrow \pi^*$ transitions which contain intra-ligand charge-transfer excitations and the lower energy band could be considered as an intra-ligand transition which possesses some MLCT character [28] [47]. This was therefore, subsequently used in the study the interactive mode of compounds **1** - **4** with CT-DNA.

Accordingly, based on the results obtained it is proposed the condensation reaction of 1,4-benzenedicarboxaldehyde and aminoethanoic acid afforded a Schiff base Ligand **L** withN_2O_2 chromophore (Figure 3). It is also suggested that ligand **L** coordinated in a tetradentate fashion, coordinating to the metal ions via its two azomethine nitrogen atoms and two oxygen atoms of its carboxylic acid end. As a consequence, it is further proposed that geometry assumed by **compound 1** is an octahedral geometry and this may be represented by Figure 4. In the case of compounds **2** and **4** a square planar is proposed. This may be depicted by Figure 5. Additionally, it is suggested that compound **3** assumed a square planar geometry; this may be represented by Figure 6.

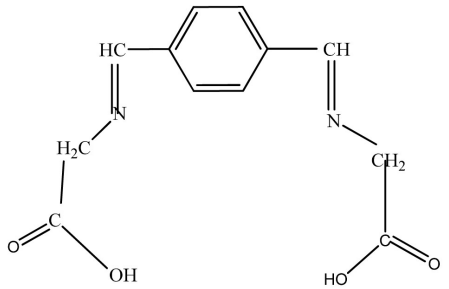

Figure 3. Ligand **L**.

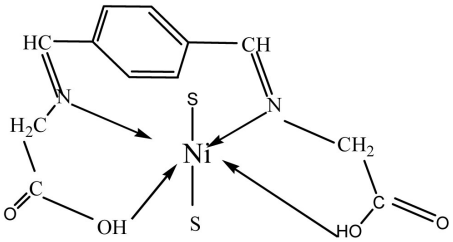

Figure 4. Compound 1; S = solvent = ethanol.

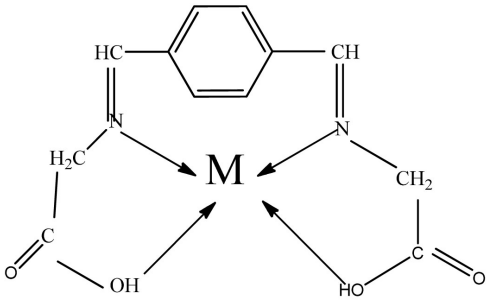

Figure 5. M = Cu/Co = compound **2**/compound **4**.

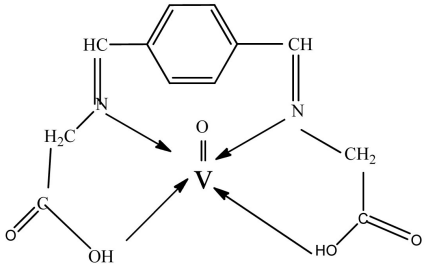

Figure 6. Compound **3**.

3.3. Antimicrobial Activity

The synthesized compounds; ligand **L** and its complexes compounds **1 - 4** were screened for their zone of inhibition against five Gram-positive and three Gram-negative bacteria and two fungi. The results obtained are presented in Table 1. The result obtained indicated that ligand **L** was inactive to all the tested organisms. Both standards **(**imipenem for bacteria and chlorhexidine for fungi) exhibited significantly better activity than all the synthesized compounds and ligand **L** ($P < 0.05$). The copper (II) complex exhibited the best activity, eliciting activity against *S. aureus*, *B. subtilis 12*, *K.pneumonia* and *P. aeruginosa*. This therefore suggests the relative broad spectrum of activity of this compound. The better activity of this compound also further validated the antimicrobial activity of copper and its complexes. All the synthesized complexes exhibited activity against *B. subtilis 12*, except the cobalt (II) complex. On the other-hand all the synthesized complexes showed moderate activity against *K. pneumonia* with exception of the nickel (II) complex. The nickel (II) and cobalt (II) complexes exhibited activity against *E. coli* a Gram negative bacteria. Although the ligand did not exhibit any antimicrobial activity, the synthesized complexes were activity against some of the microbes. This may be ascribed to the increased liposolubility of the complexes resulting in their enhanced ease of penetration through the lipid membrane of the Gram positive bacteria. As a consequence the result obtained suggests that chelation may serve as a tool for improved antimicrobial activity [23] [24] [25] [26].

3.4. Interaction with CTDNA

3.4.1. DNA Binding Using Absorption Spectroscopic Studies

Titration monitored by electronic absorption spectroscopy is one of the effective methods used in the investigation of the interaction of compounds with DNA [34]. In this present study, UV spectra of CT DNA were recorded for a constant DNA concentration ($1.2 - 1.4 \times 10^{-4}$ M) in the presence of each complex at diverse [complex]/[DNA] mixing ratios (=R). The observed increase of the absorbance of the DNA-band at λ_{max} 300 nm for compounds **1** - **4** serves to suggest the interaction of the complexes with CT-DNA [5] [28] [34]. Additionally, the UV–vis spectra of compounds **1** - **4** were recorded in the presence of increasing amounts of CT DNA. The changes of the intraligand bands located at 350 nm was monitored for compounds **1**, **2** and **4**. However the addition of CT DNA to a

Table 1. Result of zone of antimicrobial inhibition (mm) for the ligands and complexes.

	L	1	2	3	4	C
S. aureus,	-	-	09	-	-	44
S. epidermidis	-	-	-	-	-	34
B. subtilis 12	-	05	07	-	06	34
B. subtilis 82	-	-	-	-	-	29
Clostridium	-	-	-	-	-	34
K. pneumonia	-	-	04	07	08	34
P. aeruginosa	-	-	05	-	-	39
E. coli	-	05	-	-	04	33
C. albicans	-	-	-	-	-	36
C. pseudotropicalis.	-	-	-	-	-	36

Where C = imipenem and chlorhexidine for bacteria and fungi respectively.

constant solution compound **2** was monitored at λ_{max} 300 nm. The result obtained indicated hyperchromic shifts in the monitored interligand transition band for all the tested compounds. Previous studies have suggested that the binding mode of coordination compound to DNA may be either via intercalation in-between DNA-bases or by groove-binding/Coulombic forces [28] [34]. When binding is via intercalation, the orbital of the intercalated ligand can couple with the orbital of the base pairs, reducing the $\pi \rightarrow \pi^*$ transition energy and resulting in bathochromism or hypsochromism. If the coupling orbital is partially filled by electrons, it results in decreasing the transition probabilities, resulting in hyperchromism/hypochromism [5] [34]. In this study, the absorption intensities of intra-ligand charge transfer bands for compounds **1 - 4,** on addition of CT-DNA, increased significantly for each investigated compound. Additionally bathochromic shifts were observed in this band for compounds **1**, **2** and **4**. However, a blue shift was observed in the case of compound **3**. As such this suggests that the binding mode may be by intercalation. In the case of spectra obtained monitoring DNA-band with increasing concentration of complex, bathochromic shifts were observed in the $\pi \rightarrow \pi^*$ transition band of the nuclei acid. Although in some cases the observed shifts was not so pronounced. The observed shifts, therefore, serves as an indication of intercalation as the binding mode.

The values of K_b for the complexes were determined by the Wolfe Shimer equation and the corresponding plots [DNA]/($\varepsilon_a - \varepsilon_f$) versus [DNA]. The K_b values the complexes are significantly high (of the order 10^5 M^{-1}) showing that the complexes are tightly bound with CTDNA (**Table 2**). The K_b values the complexes are close and in the case of compound **1** higher than that of the classical intercalator EB ($K_b = 1.23 \times 10^5$ M^{-1}). The order for the K_b values is given as compound **1** > compound **2** > compound **4** > compound **3.** The reason for this order is not readily evident, however we suggest the structure assumed by compound 1 is the most favourably to bind to the DNA strands. Ligand **L**, however exhibited better activity when compared with the compounds **1 - 4**.

Table 2. The spectral parameters for the DNA interaction for the compounds.

Compound	λ (nm)	(ΔA/A₀) (%);	Δλ (nm)	K_b (M^{-1})
Ligand L	350	68.96 (Hyper);	+3	1.42×10^5
Compound 1	350	76.00 (Hyper);	+3	1.34×10^5
Compound 2	350	48.70 (Hyper);	+2	1.19×10^5
Compound 3	300	50.00 (Hyper);	−3	1.02×10^5
Compound 4	350	16.53 (Hyper);	+5	1.12×10^5

Where: Hyper = Hyperchromism; + red shift; − = blue shift.

3.4.2. DNA Binding Using Viscosity Measurements

In order to further clarify the nature of the interaction between the compounds **1 - 4** and CT-DNA, viscosity measurements were carried out. The relative viscosity of a DNA solution (η/η_0) is related to the relative DNA length (L/L_0) according to the equation:

$$\left(L/L_0\right) = \left(\eta/\eta_0\right)^{1/3},$$

where η_0 and L_0 denote the viscosity and the apparent molecular length in the absence of the compound, respectively [28] [33] [34]. Optical photo-physical probes provide necessary data but only sufficient evidence to support a binding mode of DNA with the complexes. Hydrodynamic methods such as viscosity measurements which are sensitive to length increase or decrease of DNA are regarded as the most effective means of studying the binding mode of complexes to DNA in the absence of crystallographic structural data and NMR [5] [34]. According to Anastasaiadou *et al.*, the presence of compounds intercalation in-between DNA-bases will lead to an increase of the DNA-bases separation distance resulting in increased relative DNA length and subsequently enhanced DNA-viscosity [28]. However on the other hand decrease DNA-viscosity suggests a relative decrease in DNA length and thus indicates that interaction with DNA is via groove-binding or Coulomb forces [28].

The changes of relative DNA-viscosity of a CT-DNA solution (0.5 mM) were monitored in the presence of increasing amounts of compounds **1** - **4** (up to the value of R = 0.5). The relative DNA-viscosity exhibited a significant increase with increasing concentration of compounds **1** - **4**. Such changes of the relative DNA viscosity may suggest the possible existence of an intercalative binding mode of the complexes in-between the DNA-bases corroborates. Additionally, the sequence of the observed increase in the values of viscosity was in positive correlation with the binding affinity to DNA.

3.4.3. DNA Binding Study Using Computational Analysis

Molecular docking has been an increasingly pivotal tool for drug discovery. The ability to predict binding affinity for different DNA target is useful in characterizing genetic regulatory pathway. This enables us to characterize the behaviour of small molecules in the binding site of target DNA as well as to elucidate fundamental biochemical processes. Molecular recognition has two important defining characteristics:

1) Specificity; which distinguishes the high specific binding partner from less specific partners;

2) Affinity; which determines that a high concentration of weakly interacting partners cannot replace the effect of a low concentration of the specific partner interacting with high affinity [55].

In view of the foregoing, the molecular docking studies of the ligand and synthesized compounds were carried out.

The ligand was prepared according to the method of Sastry G. M *et al.*, (2013) using ChemDraw 12.0 and Autodock tools software [56]. The ligand structures were drawn in 2D conformation using ChemDraw Ultra 12.0. Conversion of 2D to 3D conformation and energy minimization were carried out using Chem3D Pro 12.0. And saved in a dockable format (.pdb). The energy-minimized structure (3D conformation) was open in Autodock Tools to view the geometry and bond flexibility, and finally saved in pdbqt format. In order to estimate the conformation of the nucleic acid base-ligand complex and to increase accuracy, repeatability, and reliability of docking results, AutoDock Vina 4.2 docking program was used, as described by Jung *et al.*, 2016 [57].

AutoDock Vina is a docking program which uses the empirical scoring function and uses an iterated local search algorithm by using the search space parameters provided by the user. These include hydrogen bonding, ionic and non-polar interactions, as well as desolvation and entropic effects. The output was obtained in the form of binding energies (Kcal/mol) and the lower the energy; the more stable the protein-ligand complex. The binding conformations with the lowest binding energies were visualized in the PyMOL molecular graphics interface, and spatial (3D) and linear (2D) interaction was studied in order to know the amino acids involved in the protein-ligand complex.

Generally the result obtained indicated that the reactions were spontaneous (**Table 3**). From the result obtained ligand **L** has the least binding affinity to CT-DNA with polar contact at DC5 and DG18 residues and interaction with four residues **Figure 7** and **Figure 8**. Interestingly compound **3** demonstrated had the highest binding affinity towards CT-DNA. The compound exhibited 8.26% better affinity (−7.5 KJ/mol) for CT-DNA compared to ligand **L** (−6.2 KJ/mol). The visualization of this docked compound revealed that it had polar contact with DG2 and DA4 residues and interaction with seven residues, the highest amount to interacting sites in comparison with other synthesized compounds. This was followed by compounds **1** and **2** with both having similar polar contacts and interacting residues. The reason for observation is not readily evident to us. One potential reason for this phenomenon we propose may be that in the case of compound **3**, it is structurally more suited to interact with the observed sites. As a consequence it molecular recognition with active site in the CT-DNA was more than the others. This is indicative of its specificity for such sites in comparison with the other compounds. The binding of compound 4 with CT-DNA is illustrated in **Figure 9**, the binding of compound 4 with CT-DNA showing the interacting residue is shown in **Figure 10**.

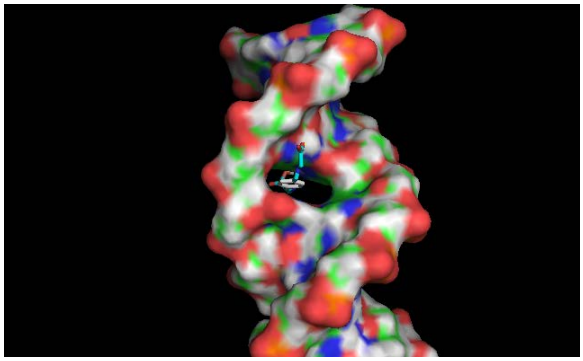

Figure 7. Binding of Ligand **L** with CT-DNA.

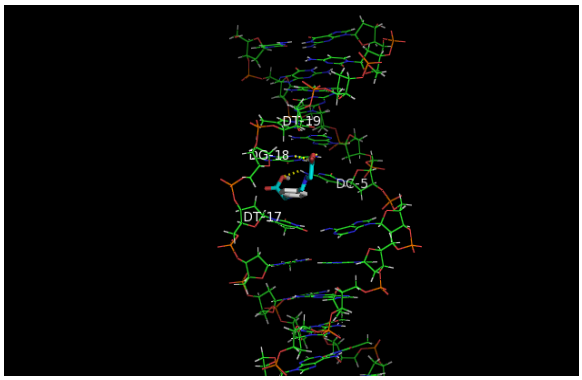

Figure 8. Binding of Ligand **L** with CT-DNA indicating the interacting residues.

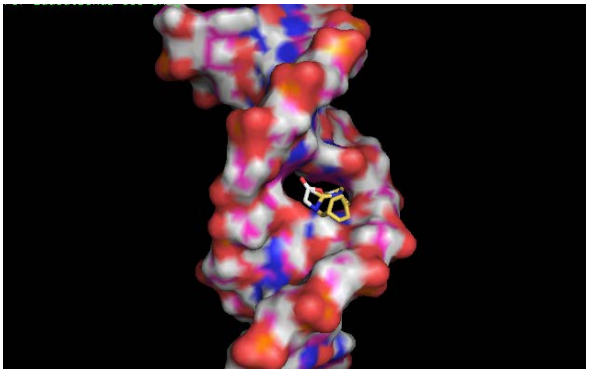

Figure 9. Binding of Compound **4** with CT-DNA.

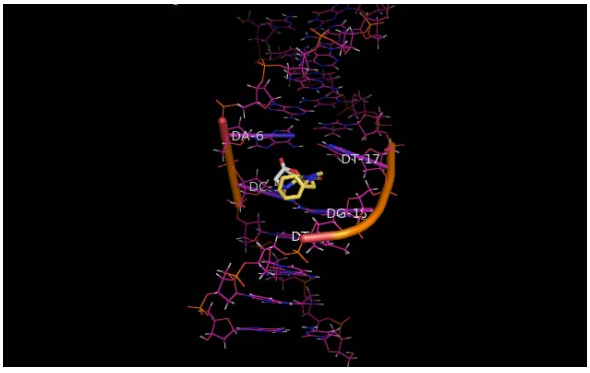

Figure 10. Binding of Compound **4** with CT-DNA showing the interacting residues.

Table 3. Binding parameters obtained from computational studies.

	Binding energy (KJ/mol)	Polar contact	Interacting Residue
Ligand L	−6.2	DC5, DG18	DC5, DT17, DG18, DT19
Compound 1	−6.8	DG2, DA4	DG2, DG3, DA4, DC5, DC20, DC21
Compound 2	−6.8	DG2, DA4	DG2, DG3, DA4, DC5, DC20, DC21
Compound 3	−7.5	DG2, DA4	DG2, DG3, DA4, DC5, DC20, DC21, DG22
Compound 4	−6.6	-	DC5, DA6, DT17, DG18, DT19

4. Conclusion

Synthesis of condensation product of 1,4-benzenedicarboxaldehyde with aminoethanoic acid and its coordination compounds **1 - 4** have been described in this study. The Schiff base was characterized using proton NMR, UV-vis and infrared spectroscopy. The coordination compounds were obtained using nickel (II), copper (II), vanady (IV) and cobalt (II) ion. The resultant coordination compounds were characterized using UV-vis and infrared spectroscopy, energy-dispersion X-ray spectroscopy EDX, EDTA complexometric titration and magnetic susceptibility. The antimicrobial activity of the compounds was determined as well as their affinity to bind to CT-DNA biomolecules. It was confirmed form characterization techniques used carboxylic acid end in the condensation product **L** and the coordination compounds **1 - 4** were protonated. The Schiff base, ligand further coordinated with metal ions in a tetradentate fashion. The involvement of the azomethine N and carboxylic acid O in bonding resulted in an N_2O_2 chromophore around the central metal atom. The results obtained are consistent with octahedral for Ni (II) complex with additional coordination with two oxygen atom of two molecules of the solvent. A square-planar geometry was suggested for both Co (II), and Cu (II) complexes and a five-coordinate, square pyramidal geometry for the VO (IV) complex. The investigated compounds in some cases exhibited moderate activity against five Gram-positive and three Gram-negative bacteria. The compounds showed nill fungicidal acidity against the two tested fungi. Compound **2** elicited the best antimicrobial activity potential. However, compound **1** had the highest affinity to CT-DNA. Generally the compounds exhibited considerable good affinity to CT-DNA.

Acknowledgements

The Laboratory for Analytical Services, Research Focus Area for Chemical Resource Beneficiation, Potchefstroom, South Africa is acknowledged for provision of NMR facilities.

Author Contributions

All the authors contributed to the conceptualization and critical revisions of the

work and T.O. compiled the original draft.

Conflicts of Interest

The authors declare no conflict of interest.

References

[1] Lu, J.W., Huang, Y.H., Lo, S.I. and Wein, H.H. (2007) New μ-Oxo-Bridged Tetranuclear Cu(II) Complex with Schiff-Base Ligand: Synthesis, Crystal Structure and Magnetic Properties. *Inorganic Chemistry Communications*, **10**, 1210-1213. https://doi.org/10.1016/j.inoche.2007.07.009

[2] Cozzi, P.G., Dolci, L.S., Garelli, A., Montalti, M., Prodi, L. and Zaccheroni, N. (2003) Photophysical Properties of Schiff-Base Metal Complexes. *New Journal of Chemistry*, **27**, 692-697. https://doi.org/10.1039/b209396k

[3] Morris, G.A., Zhou, H., Stern, C.L. and Nguyen, S.T. (2001) A General High-Yield Route to Bis(salicylaldimine) Zinc(II) Complexes: Application to the Synthesis of Pyridine-Modified Salen-Type Zinc(II) Complexes. *Inorganic Chemistry*, **40**, 3222-3227. https://doi.org/10.1021/ic010090o

[4] Rajavel, N.M. (2014) Synthesis, Spectroscopic, DNA Cleavage and Antibacterial Activity of Binuclear Schiff Base Complexes. *Arabian Journal of Chemistry*, **7**, 509-517. https://doi.org/10.1016/j.arabjc.2010.11.010

[5] Abdel-Rahman, L.H., El-Khatib, R.M., Nassr, L.A.E. and Abu-Dief, A.M. (2013) Synthesis, Physicochemical Studies, Embryos Toxicity and DNA Interaction of Some New Iron(II) Schiff Base Amino Acid Complexes. *Journal of Molecular Structure*, **1040**, 9-18. https://doi.org/10.1016/j.molstruc.2013.02.023

[6] Atkins, R., Breweg, G., Kakot, E., Mockler, G.M. and Sinn, E. (1985) Copper(II) and Nickel(II) Complexes of Unsymmetrical Tetradentate Schiff Base Ligands. *Inorganic Chemistry*, **24**, 127-134. https://doi.org/10.1021/ic00196a003

[7] Yuan, R., Chai, Y., Liu, D., Gao, D., Li, J. and Yu, R. (1993) Schiff Base Complexes of Cobalt(II) as Neutral Carriers for Highly Selective Iodide Electrodes. *Analytical Chemistry*, **65**, 2572-2575. https://doi.org/10.1021/ac00067a005

[8] Ramesh, R., Saganthy, P.K. and Natarajan, K. (1996) Synthesis, Spectra and Electrochemistry of Ru(III) Complexes with Tetradentate Schiff Bases. *Synthesis and Reactivity in Inorganic and Metal-Organic Chemistry*, **26**, 47-60. https://doi.org/10.1080/00945719608004245

[9] Ohashi, Y. (1997) Excitation Energy Dependence of Transient Absorptions of [N,N'-Phenylenebis(Salicylideneaminato)] Cobalt(II) in Dmf Solution. *Bulletin of the Chemical Society of Japan*, **70**, 1319-1324. https://doi.org/10.1246/bcsj.70.1319

[10] Shelke, V.A., Jadhav, S.M., Patharkar, V.R., Shankarwar, S.G., Munde, A.S. and Chondhekar, T.K. (2012) Synthesis, Spectroscopic Characterization and Thermal Studies of Some Rare Earth Metal Complexes of Unsymmetrical Tetradentate Schiff Base Ligand. *Arabian Journal of Chemistry*, **5**, 501-507. https://doi.org/10.1016/j.arabjc.2010.09.018

[11] Flaih, H., Al-Jeboori, T.A.M., Al-Shimiesawi Oun, A.Y., *et al.* (2014) Synthesis and Characterization of Amino Acid (Phenylalanine) Schiff Bases and Their Metal Complexes. *Journal of Chemical and Pharmaceutical Research*, **6**, 44-53,

[12] Wang, M.Z., Meng, Z.X., Liu, B.L., Lai, C.G., Zhang, C.L. and Wang, X.Y. (2005) Novel Tumo Chemotherapeutic Agents and Tumor Radio-Imaging Agents: Potential Tumor Pharmaceuticals of Tenary Copper(II) Complexes. *Inorganic Chemistry*

Communications, **8**, 368-504. https://doi.org/10.1016/j.inoche.2005.01.023

[13] Wang, G. and Chang, J.C. (1994) Synthesis and Characterization of Amino Acid Schiff Base Complexes of Nickel(II). *Synthesis and Reactivity in Inorganic and Metal-Organic Chemistry*, **24**, 1091-1097. https://doi.org/10.1080/00945719408001385

[14] Wang, G. and Chang, J.C. (1994) Copper(II) and Zinc(II) Complexes of Schiff Bases Derived from Amino Acids and O-Vanillin. *Synthesis and Reactivity in Inorganic and Metal-Organic Chemistry*, **24**, 623-630. https://doi.org/10.1080/00945719408000138

[15] Erkkila, K.E., Odom, D.T. and Barton, J.K. (1999) Recognition and Reaction of Metallointercalators with DNA. *Chemical Reviews*, **9**, 2777-2796. https://doi.org/10.1021/cr9804341

[16] Vijayalakshmi, R., Kanthimathi, M., Subramanian, V. and Nair, B.N. (2000) DNA Cleavage by a Chromium(III) Complex. *Biochimica et Biophysica Acta*, **1475**, 157-162.

[17] He, J., Sun, J., Mao, Z.W., Ji, L.N. and Sun, H. (2009) Phosphodiester Hydrolysis and Specific DNA Binding and Cleavage Promoted by Guanidinium-Functionalized Zinc Complexes. *Journal of Inorganic Biochemistry*, **103**, 851-858. https://doi.org/10.1016/j.jinorgbio.2009.02.010

[18] Wang, X.Y., Zhang, J., Li, K., Jiang, N., Chen, S.Y., Lin, H.H., Huang, Y., Ma, L.J. and Yu, X.Q. (2006) Synthesis and DNA Cleavage Activities of Mononuclear Marocyclic Polyamine Zinc(II), Copper(II), Cobalt(II) Complexes which Linked with Uracil. *Bioorganic & Medicinal Chemistry*, **14**, 6745-6751. https://doi.org/10.1016/j.bmc.2006.05.049

[19] Abdel-Rahman, L.H., El-Khatib, R.M., Nassr, L.A.E., Abu-Dief, A.M. and El-DinLashin, F. (2013) Design, Characterization, Teratogenicity Testing, Antibacterial, Antifungal and DNA Interaction of Few High Spin Fe(II) Schiff Base Amino Acid Complexes. *Spectrochimica Acta Part A*: *Molecular and Biomolecular Spectroscopy*, **111**, 266-276. https://doi.org/10.1016/j.saa.2013.03.061

[20] Dehkordi, M.N., Bordbar, A., Lincoln, P. and Mirkhani, V. (2012) Spectroscopic Study on the Interaction of ct-DNA with Manganese Salen Complex Containing Triphenylphosphonium Groups. *Spectrochimica Acta Part A*: *Molecular and Biomolecular Spectroscopy*, **90**, 50-54. https://doi.org/10.1016/j.saa.2012.01.015

[21] Ferell, N.P. (2003) Metal Complexes as Drugs and Chemotherapeutic Agents. In: *Comprehensive Coordination Chemistry II*, Elsevier, Amsterdam, Vol. 9, 809-847. https://doi.org/10.1016/B0-08-043748-6/09021-6

[22] Sakurai, H., Yoshikawa, Y., Kawabe, K. and Yasui, H. (2002) Antidiabetic Vanadium(IV) and Zinc(II) Complexes. *Coordination Chemistry Reviews*, **226**, 187-198. https://doi.org/10.1016/S0010-8545(01)00447-7

[23] Chang, E., Simmers, C. and Knight, A. (2010) Cobalt Complexes as Antiviral and Antibacterial Agents. *Pharmaceuticals*, **3**, 1711-1728. https://doi.org/10.3390/ph3061711

[24] Chohan, Z.H., Arif, M., Akhtar, M.A. and Supurean, C.T. (2006) Metal-Based Antibacterial and Antifungal Agents: Synthesis, Characterization and *in Vitro* Biological Evaluation of Co(II), Cu(II), Ni(II), and Zn(II) Complexes with Amino Acid-Derived Compounds. *Bioinorganic Chemistry and Application*, **13**, 831-837. https://doi.org/10.1155/BCA/2006/83131

[25] Sadlers, P., Muncia, C. and Shipman, M.A. (2007) Metals in Medicine. In: Bertini, I., Gray, H., Stiefel, E. and Valentine, J., Eds., *Biological Inorganic Chemistry*: *Structure and Reactivity*, University Science Books, London, 115-136.

[26] Chohan, Z.H., Farooq, M.A., Scozzafava, A. and Supuran, C.T. (2002) Antibacterial Schiff Bases of Oxalyl-Hydrazine; Diamide Incorporating Pyrrolyl and Salicylyl Moieties and of Their Zinc(II) Complexes. *Journal of Enzyme Inhibition and Medicinal Chemistry*, **17**, 1-7. https://doi.org/10.1080/14756360290005598

[27] Đuri, S.Z., Vojnovic, S., Andrejevi, T.P., Stevanovi, N.L., Savi, N., Nikodinovic-Runic, J., *et al.* (2020) Antimicrobial Activity and DNA/BSA Binding Affinity of Polynuclear Silver(I) Complexes with 1,2-Bis(4-pyridyl)ethane/ethene as Bridging Ligands. *Bioinorganic Chemistry and Application*s, **2020**, Article ID: 3812050. https://doi.org/10.1155/2020/3812050

[28] Anastasiadoua, D., Psomasa, G., Kalogiannis, S., Geromichalosa, G., Hatzidimitrioua, A.G. and Aslanidisa, P. (2019) Bi- and Trinuclear Copper(I) Compounds of 2,2,5,5-tetramethyl-imidazolidine-4-thione and 1,2-bis(diphenylphosphano)ethane: Synthesis, Crystal Structures, *in Vitro* and *in Silico* Study of Antibacterial Activity and Interaction with DNA and Albumins. *Journal of Inorganic Biochemistry*, **198**, Article ID: 110750. https://doi.org/10.1016/j.jinorgbio.2019.110750

[29] Patel, S.H., Parekh, H.M., Panchal, P.K. and Patel, M.P. (2007) Polymeric Coordination Compounds Derived from Transition Metal(II) with Teradentate Schiff-Base: Synthetic, Spectroscopic, Magnetic and Thermal Approach. *Journal of Macromolecular Science*, *Part A*: *Pure and Applied Chemistry*, **44**, 599-603. https://doi.org/10.1080/10601320701284881

[30] Borisova, N.E., Reshetova, M.D. and Ustynyuk, Y.A. (2007) Metal-Free Methods in the Synthesis of Macrocyclic Schiff Bases. *Chemical Reviews*, **107**, 46-79. https://doi.org/10.1021/cr0683616

[31] Chatterjee, D. and Mitra, A. (2003) Synthesis, Characterization and Reactivities of Schiff-Base Complexes of Ruthenium(III). *Journal of Coordination Chemistry*, **57**, 175-182. https://doi.org/10.1080/00958970410001662435

[32] Aiyelabola, T.O., Ojo, I.A.O. and Akinkunmi, E.O. (2012) Structural and Antimicrobial Studies of Coordination Compounds of Phenylalanine and Glycine. *International Journal of Chemistry*, **4**, 49-59. https://doi.org/10.5539/ijc.v4n2p49

[33] Raman, N., Pothiraj, K. and Baskaran, T. (2011) DNA Interaction, Antimicrobial, Electrochemical and Spectroscopic Studies of Metal(II) Complexes with Tridentate Heterolytic Schiff Base Derived from 2'-Methylacetoacetanilide. *Journal of Molecular Structure*, **1000**, 135-144. https://doi.org/10.1016/j.molstruc.2011.06.006

[34] Abdel-Rahman, L.H., El-Khatib, R.M., Nassr, L.A.E. and Abu-Dief, A.M. (2017) DNA Binding Ability Mode, Spectroscopic Studies, Hydrophobicity, and *in Vitro* Antibacterial Evaluation of Some New Fe(II) Complexes Bearing ONO Donor Amino Acid Schiff Bases. *Arabian Journal of Chemistry*, **10**, S1834-S1846. https://doi.org/10.1016/j.arabjc.2013.07.010

[35] Gou, Y., Li, J., Fan, B., Xu, B., Zhou, M. and Yang, F. (2017) Structure and Biological Properties of Mixed-Ligand Cu(II) Schiff Base Complexes as Potential Anticancer Agents. *European Journal of Medicinal Chemistry*, **134**, 207-217. https://doi.org/10.1016/j.ejmech.2017.04.026

[36] Sabolová, D., Kožurková, M., Plichta, T., Ondrušová, Z., *et al.* (2011) Interaction of a Copper(II)-Schiff Base Complexes with Calf Thymus DNA and Their Antimicrobial Activity. *International Journal of Biological Macromolecules*, **48**, 319-325. https://doi.org/10.1016/j.ijbiomac.2010.12.001

[37] Satyanarayana, J.C. and Chaires, J.B. (1992) Neither .DELTA. - nor .LAMBDA. -tris(Phenanthroline)Ruthenium(II) Binds to DNA by Classical Intercalations. *Biochemistry*, **31**, 9319-9324. https://doi.org/10.1021/bi00154a001

[38] Pavia, D., Lampman, G. and Kriz, G. (2001) Introduction to Spectroscopy, a Guide for Students of Organic Chemistry. 3rd Edition, Brooks and Cole, Washington, 22-368.

[39] Kemp, W. (1999) Organic Spectroscopy. 3rd Edition, Macmillan, Hong Kong, 19-98.

[40] Saunders, J.K.M. and Hunters, B.K. (1992) Modern NMR Spectroscopy a Guide for Chemists. 2nd Edition, Oxford University Press, London, 34-95.

[41] Gunther, H. (1995) NMR Spectroscopy, Basic Principles, Concepts and Applications in Chemistry. 2nd Edition, John Wiley and Sons, New York, 1-78.

[42] Nakamoto, K. (2009) Infrared and Raman Spectroscopy of Inorganic and Coordination Compounds: Applications in Coordination, Organometallics and Bioinorganic Chemistry. 6th Edition, John Wiley and Sons, New York, 67-69.

[43] Perkampus, H. (1992) Analytical Application of UV-Vis. 2nd Edition, Springer, Berlin, 26-80. https://doi.org/10.1007/978-3-642-77477-5_4

[44] Bellamy, L.J. (1976) The Infrared Spectra of Complex Molecules. Chapman and Hall, London, 1-190.

[45] Stuart, B.H. (2004) Infrared Spectroscopy Fundamentals and Applications. John Wiley and Sons Ltd., West Sussex, 1-110. https://doi.org/10.1002/0470011149

[46] Miessler, G.L. and Tarr, D.A. (1999) Inorganic Chemistry. Pearson Prentice Hall, New York, Vol. 642, 315-316.

[47] Greenwood, N.N. and Earnshaw, A. (1997) Chemistry of the Elements. 2nd Edition, Butterworth-Heinemann, Hong Kong, 1060-1090, 1290-1326.

[48] Osowole, A.A., Kolawole, O.E. and Fagade, S. (2008) Synthesis Physicochemical and Biological Properties of Nickel(II), Copper(II) and Zinc(II) Complexes of an Unsymmetrical Tetradentate Schiff Base and Adducts with 2,2'-Dipyridine and 1,10-Phenantroline. *Journal of Coordination Chemistry*, **61**, 1046-1055. https://doi.org/10.1080/00958970701482446

[49] Osowole, A. (2011) Synthesis, Characterization and Magnetic and Thermal Studies on Some Metal(II) Thiophenyl Schiff Base Complexes. *International Journal of Inorganic Chemistry*, **2011**, Article ID: 650186. https://doi.org/10.1155/2011/650186

[50] Youssef, N.S. and Hegab, K.H. (2005) Synthesis and Characterization of Some Transition Metal Complexes of Thiosemicarbazones Derived from 2-Acetylpyrrole and 2-Acetylfuran. *Synthesis and Reactivity in Inorganic*, *Metal Organic*, *and Nano Metal Chemistry*, **35**, 391-399.

[51] Xiu, R.B., Mintz, F.L., You, X.Z., Wang, R.X., Yue, Q., Meng, Q.J., Lu, Y.J. and Derveer, D.V. (1996) Synthesis and Characterization of Vanadyl Complexes with Unsymmetrical Bis-Schiff Base Ligands Containing a cis-N2O2 Coordinate Chromophore. *Polyhedron*, **15**, 4585-4591. https://doi.org/10.1016/0277-5387(96)00220-3

[52] Nejo, A.A., Kolawole, G.A., Opoku, A.R., Muller, C. and Wolowska, J. (2009) Synthesis, Characterization and Insulin-Enhancing Studies of Unsymmetrical Tetradentate Schiff-Base Complexes of Oxovanadium. *Journal of Coordination Chemistry*, **62**, 3411-3424. https://doi.org/10.1080/00958970903104327

[53] Aiyelabola, T.O., Akinkunmi, E., Ojo, I., Obuotor, E., Adebajo, C. and Isabirye, D. (2017) Syntheses, Characterization, Resolution and Biological Studies of Coordination Compounds of Aspartic Acid and Glycine. *Bioinorganic Chemistry and Applications*, **2017**, Article ID: 2956145. https://doi.org/10.1155/2017/2956145

[54] Anitha, C., Sheela, C.D., Tharmaraj, P. and Shanmugakala, R. (2013) Studies on Synthesis and Spectral Characterization of Some Transition Metal Complexes of Azo-Azomethine Derivative of Diaminomaleonitrile. *International Journal of Inor-*

ganic Chemistry, **2013**, Article ID: 436275. https://doi.org/10.1155/2013/436275

[55] Du, X., Li, Y., Xia, Y., *et al.* (2016) Insights into Protein-Ligand Interactions: Mechanisms, Models, and Methods. *International Journal of Molecular Science*, **17**, 144. https://doi.org/10.3390/ijms17020144

[56] Sastry, G.M., Adzhigirey, M., Day, T., Annabhimoju, R. and Sherman, N. (2013) Protein and Ligand Preparation: Parameters, Protocols, and Influence on Virtual Screening Enrichments. *Journal of Computer-Aided Molecular Design*, **27**, 221-234. https://doi.org/10.1007/s10822-013-9644-8

[57] Shivanika, C., Deepak Kumar, S., Ragunathan, V., Tiwari, P., Sumitha, A. and Brindha, D.P. (2020) Molecular Docking, Validation, Dynamics Simulations, and Pharmacokinetic Prediction of Natural Compounds against the SARS-CoV-2 Main-Protease. *Journal of Biomolecular Structure and Dynamics*. https://doi.org/10.1080/07391102.2020.1815584